Materials Today: Proceedings xxx (xxxx) xxx

Contents lists available at ScienceDirect

Materials Today: Proceedings

journal homepage: www.elsevier.com/locate/matpr

Frequency and temperature-dependent dielectric characteristics of lead-free Br doped perovskites $(CH_3NH_3)_3Bi_2Cl_9$ and $(CH_3NH_3)_3Bi_2Br_xCl_{9-x}$

Paramesh Chandra, Saroj Saha, Swapan K. Mandal *

Department of Physics, Visva-Bharati, Santiniketan 731235, India

ARTICLE INFO

Article history:
Available online xxxx

Keywords:
Perovskite
Chemical synthesis
Impedance spectroscopy
Dielectric relaxation
Doping

ABSTRACT

We report the synthesis and dielectric characteristics of lead-free methylammonium bismuth chloride (MABiCl) and Br doped methylammonium bismuth chloride (MABiBrCl) in powder form. The morphology of the samples showed growth of large flakes with large surface area. The band gaps of the perovskites are obtained from optical absorption data. The dielectric characteristics of the samples were measured in the frequency range 1 Hz to 1 MHz and temperature range 100–300 K. The data shows a complex electrical transport in these halide perovskite materials. The dielectric permittivity data shows the existence of a critical temperature at which the material undergoes a structural phase transition. The transition temperature is found to be 270 K and 266 K for MABiCl and MABiBrCl respectively. The results can be explained by certain change in orientation of methyl-ammonium (MA) ions as the temperature is increased.

Selection and peer-review under responsibility of the scientific committee of the Condensed Matter Physics.

1. Introduction

The halide perovskites, particularly hybrid organic–inorganic ABX_3 type perovskites (A = organic cation, B = inorganic metal, and X = halogen) have gained much attention as light-harvesting materials in thin-film photovoltaics. Because of their superior light-absorption properties, charge-transport dynamics, and their simple solution-based fabrication methods[1–7], the amount of research work is steadily increasing. The lead-based hybrid perovskite achieved its maximum efficiency of 25.8% [8]. However, lead-based PSCs face significant challenges of lead poisoning, the instability that leads to roadblocks to the successful commercialization of lead-based PSCs [9]. Therefore, it has always been a researcher's goal to find a suitable lead-free perovskite with similar photovoltaic characteristics. The two most tested metals instead of lead are Sn and Ge. In comparison with conventional organic–inorganic hybrid perovskite $MAPbI_3$, Sn and Ge compounds have many similarities in terms of photoelectric and photosensitive properties. The Sn perovskite $CH_3NH_3SnI_3$ has achieved a moderate PCE (more than 6%)[10]. However, Sn^{2+} can easily be oxidized to Sn^{4+}, resulting in instability [11–13]. For Ge-based perovskite, it is difficult to stabilize the perovskite phase for solar cell fabrication [14]. As a result, Ge-based PSCs exhibit low optical current density and PCE (0.2%). One of the most promising cation to replace Pb^{2+}(electron configuration [Xe] ($4f^{14}5d^{10}$ 6 s^2 $6p^2$)) is Bi^{3+} (electron configuration [Xe] ($4f^{14}$ $5d^{10}$ 6 s^2 $6p^3$)) with similar electronic configuration and ionic radii, and with better stability [15,16]. Recent studies have shown that the $(CH_3NH_3)_3Bi_2Cl_9$ (MABiCl) bismuth-based compound [17,18] can be used as a precursor for visible absorption in solar cells. The presence of pair of 6 s^2 electrons can be a possible reason for a more stable perovskite structure. Also, the non-toxic property of MABiCl is a great advantage to go forward with this material. Charge transport of undoped semiconductors is mostly dominated by intrinsic excitation, generated by external factors like temperature, but the number of charge carriers remains small. Mixing of a different halogen may trigger new charge carrier generation, and also it may modify the rotation of ions present in the perovskite structure [19–22]. We studied here the dielectric, optical, structural and morphological characteristics of MABiCl and MABiBrCl powder.

2. Experimental details

2.1. Chemicals

The starting materials for the synthesis of perovskite material were methylamine, hydrochloric acid (HCl, Merck Chemicals), hydrobromic acid (HBr, Merck Chemicals), anhydrous N, N dimethylformamide (DMF) (C_3H_7NO, Merck Chemicals, 99.5%). All

* Corresponding author.
E-mail address: sk_mandal@hotmail.com (S.K. Mandal).

https://doi.org/10.1016/j.matpr.2022.06.413
2214-7853/
Selection and peer-review under responsibility of the scientific committee of the Condensed Matter Physics.

the chemicals were taken of analytical grade purity and procured from commercial sources and no further purification was performed.

2.2. MABiCl synthesis

The precursor CH_3NH_3Cl (MACl) are prepared by reacting 1:1 ratio of methylamine (33 wt% in ethanol) and hydrochloric acid (35%) in absolute ethanol in an ice bath for 2 h under controlled conditions. We observed a transparent solution, which we let evaporate slowly almost for 24 h, maintained at 50 °C. After the ethanol was completely evaporated, a white precipitate of MACl was observed.

The end product, lead-free Bi-based perovskite $(CH_3NH_3)_3Bi_2Cl_9$ (MABiCl) was obtained by mixing 3:2 M amount CH_3NH_3Cl (10 mMol) and $BiCl_3$ (6.66 mMol) in DMF. The solution was stirred for half an hour at 50 °C and finally a translucent white colloidal solution was obtained. 20 ml of ethyl alcohol is added to get a white precipitate. The solution is filtered and dried under a constant 60 °C under vacuum obtain MABiCl white powder.

2.3. MABiBrCl synthesis

The precursor CH_3NH_3Br (MABr) are prepared by reacting 1:1 ratio of methylamine (33 wt% in ethanol) and hydrochloric acid (35%) in absolute ethanol in an ice bath for 2 h under controlled conditions. We observed a transparent yellow solution, which we let evaporate slowly almost for 24 h, keeping the bath temperature at 50 °C. After the ethanol was completely evaporated, a yellow precipitate of MABr was observed.

The Br dopped Bi-based perovskite $(CH_3NH_3)_3Bi_2Br_3Cl_6$ (MABiBrCl) was done by mixing 3:2 M amount CH_3NH_3Br (10 mMol) and $BiCl_3$ (6.66 mMol) in DMF. The solution is kept in stirring condition for half an hour at 50 °C resulting in a yellow foggy solution. Addition of 20 ml ethyl alcohol resulted in a white precipitate. The solution was filtered and dried at a constant temperature of 60 °C under vacuum to obtain a yellow MABiBrCl powder.

2.4. Material characterization

Scanning electron microscopy (SEM ZEISS GEMINI SEM 450) with energy dispersive x-ray (EDX) facility was used to study the morphology and chemical composition of the MABiCl and MABiBrCl samples. To measure the complex impedance, the pellet of MABiCl and MABiBrCl samples has been kept between two copper electrodes, and all data have been recorded using Hioki LCR Q (LM3536) meter. The crystal structure of the sample is obtained by synchrotron X-ray diffraction (INDUS-II Grazing Incidence X-ray Scattering (GIXS) Beam Line No.-13, RRCAT Indore). A scintillation detector (C400, Oxford Instruments) is attached to the goniometer's detection arm with a crossed slit assembly. Optical properties were measured with Beckman Coulter DU720 UV–Vis spectrometer.

3. Results and discussion

3.1. Crystal structure

Fig. 1 (b) shows the XRD pattern of the precursor MABiCl crystal, and the characteristic diffraction peaks are compared with those of calculated XRD pattern from the CIF (Crystallographic Information file) of the previously published literature [17] which is depicted in Fig. 1 (a). Fig. 1 (c) shows the XRD pattern of MABiBrCl powder. It can be seen from the XRD spectrum that diffraction peaks appear at 7.89°, 8.82°, 10.59°, 13.96°, 15.96°, 17.30°, 22.08°, 31.97°, 35.10°, and 37.99°, respectively. The corresponding crystal indices are (101), (200), (201), (111), (202), (400), (312), (422), (800) and (331). It indicates that the crystal structure of the prepared organic–inorganic hybrid perovskite films is monoclinic with P21/n symmetry. For the doped samples, two additional peaks at 60.63° and 63.52° are obtained. The additional peaks observed may arise due to unreacted bismuth phase in the sample [23,24].

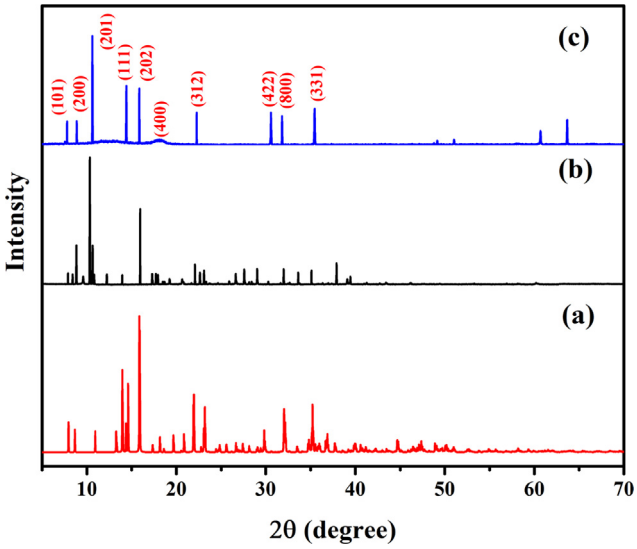

Fig. 1. X-Ray diffraction plot for (a) calculated from the CIF (a) $(CH_3NH_3)_3Bi_2Cl_9$ (MABiCl) and **(b)** $(CH_3NH_3)_3Bi_2Br_xCl_{9-x}$ (x = 3) (MABiBrCl).

3.2. Optical studies

Optical absorption data is shown in Fig. 2. The bandgaps are calculated from the optical absorption data are 2.65 and 2.70 eV for MABiCl and MABiBrCl respectively. The absorption curves are quite similar for both the samples. Slight increase (50 meV) in bandgap is observed for the Br doped sample. Conventionally, the band gap decreases in perovskites when the ionic radius of the halogen ion increases but we observed a slight discrepancy in our result where bandgap increases with Br doping. This anomaly may be explained due to size effect of the perovskites flakes. Dependence of optical

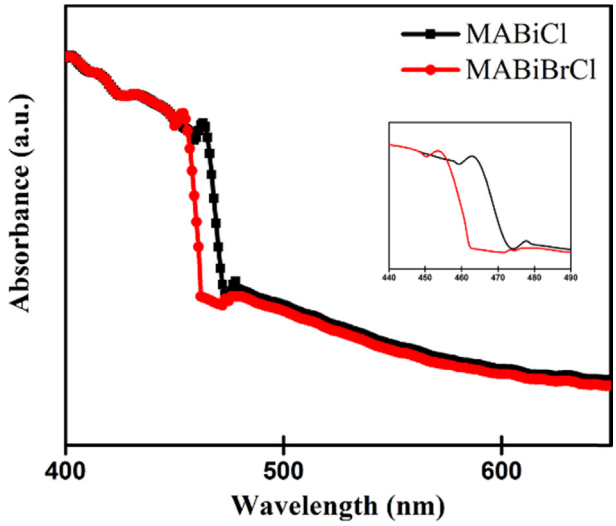

Fig. 2. Optical absorption data for MABiCl and MABiBrCl samples.

absorbance with the particle size of the sample is an observed phenomenon [25]. Introduction of Br during synthesis plausibly resulted in a reduction of particle (flake) size (as seen in FESEM images) and hence the blue-shift of absorption peak and increase in band gap energy.

3.3. FESEM analysis

The morphological structure of MABiCl and MABiBrCl samples is shown in Fig. 3(a) and Fig. 3(b), respectively. It is observed that the microstructure contains disc-like flakes ranging from 100 nm to 5 μm. The EDX spectra of the samples as shown in Fig. 3 (c), (d) confirm the presence of constituent elements (C, N, Cl, Br, Bi). The distribution of flakes was more uniform for Br doped than the MABiCl sample.

4. Dielectric permittivity

The frequency dependent dielectric behaviour of MABiCl and MABiBrCl can be studied by the complex permittivity. The complex dielectric permittivity can be expressed as:

$$\varepsilon(\omega) = \varepsilon'(\omega) - j\varepsilon''(\omega)$$

where the real part $\varepsilon\prime(\omega)$ is defined as charge storing capacity and the imaginary part $\varepsilon\prime\prime(\omega)$ represents the energy loss within the material [26–30].

Unlike insulators where the relaxation mechanism is mostly influenced by the frequency-dependent part of the impedance value, semiconductors consist of frequency-independent DC conductivity, which complicates the analysis of any relaxation process [31–33]. Fig. 4 (a) and (c) shows the variation of $\varepsilon'(\omega)$ with temperature for sample MABiCl and MABiBrCl respectively and Fig. 4 (b) and (d) shows the variation of dielectric loss $\varepsilon\prime\prime(\omega)$ with temperature for different frequencies. We have observed a sudden leap of $\varepsilon'(\omega)$ at temperature $\sim$ 270 K and $\sim$ 266 K for MABiCl and

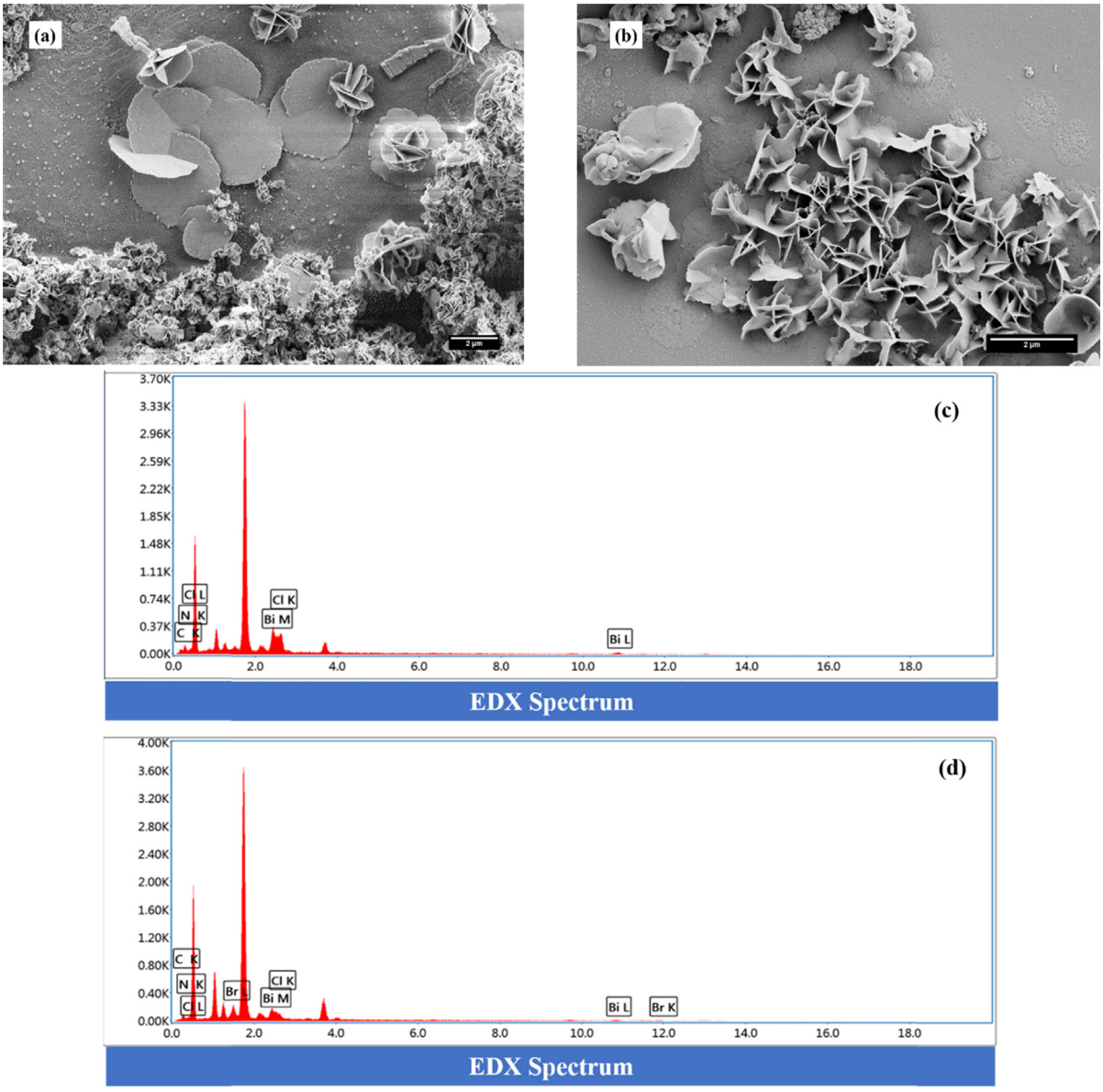

Fig. 3. SEM image of **(a)** $(CH_3NH_3)_3Bi_2Cl_9$ (MABiCl) and **(b)** $(CH_3NH_3)_3Bi_2Br_xCl_{9-x}$ (x = 3) (MABiBrCl). The SEM showed growth of disc-shaped flakes for both the samples. EDX spectra are shown in (c) MABiCl and (d) MABiBrCl respectively.

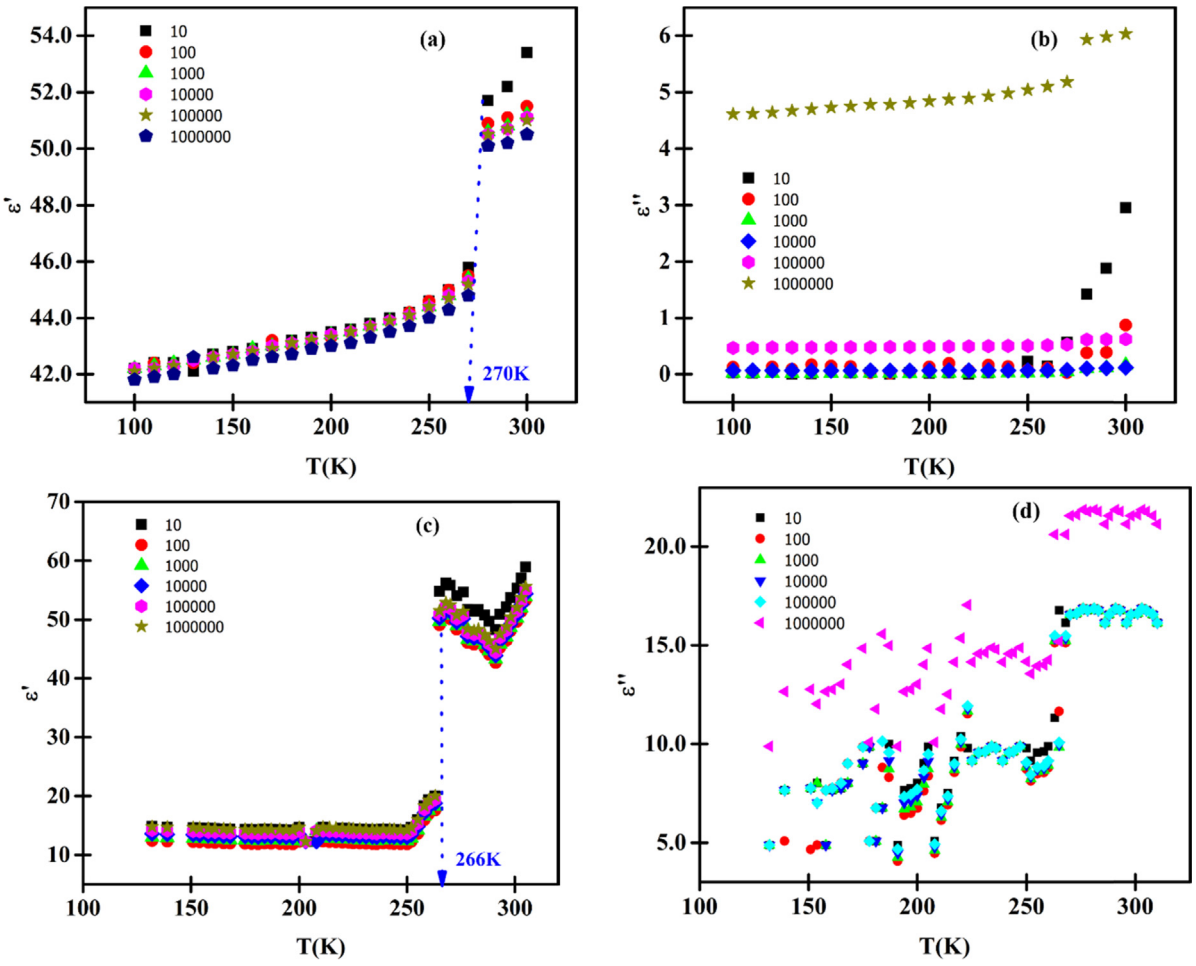

Fig. 4. The temperature-dependent plot of the real and imaginary parts of dielectric permiitivity at different frequencies, (a) real part ε′(ω) and (b) imaginary part ε″(ω) MABiCl sample. (c) real part ε′(ω) and (d) imaginary part ε″(ω) for MABiBrCl.

MABiBrCl, respectively. This plausibly results from a structural phase transition as reported by Belkyal *et al.* from XRD data [34]. The MA ion present inside the structure is disordered in orientations relative to the rotation around the C-N axis. The permittivity value is almost constant below a specific temperature. When a critical temperature is reached, the MA ions achieve a new rotational degree of freedom and change the intrinsic crystal structure of the samples. We find that the critical temperature of transition is lower for Br doped sample. So, doping may be a viable option to tweak the transition temperature for any practical purpose. The samples exhibit a slight dielectric loss at higher frequencies as shown in Fig. 4(b) and (d).

5. Conclusion

In summary, dielectric behaviours of MABiCl and MABiBrCl samples at 100–300 K are reported here. We observed that the crystallinity of the samples was largely unaffected by doping. The dielectric studies indicated a sharp change in permittivity at a particular critical temperature 270 K and 266 K for MABiCl and MABiBrCl respectively. This can be related to a change in the orientation of the MA ions giving rise to a structural phase transition which is dependent on temperature. The studies performed here are in agreement with the proposed model in which the rotational motion of MA ions around the C-N axis and its temperature dependence were considered [35].

Data availability

Data will be made available on request.

Declaration of Competing Interest

The authors declare that they have no known competing financial interests or personal relationships that could have appeared to influence the work reported in this paper.

Acknowledgments

Saroj Saha acknowledges with thanks to CSIR, Govt. of India for providing Senior Research Fellowship. UGC-DAE, Indore is acknowledged with thanks for providing dielectric measurement facilities.

Data availability

The author acknowledges that all data generated and analysed during this study were included in this paper. In addition, all sources used in connection with the study were appropriately referenced or publicly available at the time of submission.

References

[1] A. Kojima, K. Teshima, Y. Shirai, T. Miyasaka, Organometal halide perovskites as visible-light sensitizers for photovoltaic cells, J. Am. Chem. Soc. 131 (2009) 6050–6051, https://doi.org/10.1021/ja809598r.

[2] J.M. Azpiroz, E. Mosconi, J. Bisquert, F. De Angelis, Defect migration in methylammonium lead iodide and its role in perovskite solar cell operation, Energy Environ. Sci. 8 (2015) 2118–2127, https://doi.org/10.1039/c5ee01265a.

[3] T.Y. Yang, G. Gregori, N. Pellet, M. Grätzel, J. Maier, The Significance of Ion Conduction in a Hybrid Organic-Inorganic Lead-Iodide-Based Perovskite Photosensitizer, Angew. Chem. – Int. Ed. 54 (2015) 7905–7910, https://doi.org/10.1002/anie.201500014.

[4] S.S. Shin, E.J. Yeom, W.S. Yang, S. Hur, M.G. Kim, J. Im, J. Seo, J.H. Noh, S.I. Seok, Colloidally prepared La-doped BaSnO 3 electrodes for efficient, photostable perovskite solar cells, Science 356 (2017) 167–171, https://doi.org/10.1126/science.aam6620.

[5] Q. Jiang, L. Zhang, H. Wang, X. Yang, J. Meng, H. Liu, Z. Yin, J. Wu, X. Zhang, J. You, Enhanced electron extraction using SnO2 for high-efficiency planar-structure HC(NH2)2 PbI3-based perovskite solar cells, Nat. Energy 2 (2017) 16177, https://doi.org/10.1038/nenergy.2016.177.

[6] T. Jesper Jacobsson, J.P. Correa-Baena, M. Pazoki, M. Saliba, K. Schenk, M. Grätzel, A. Hagfeldt, Exploration of the compositional space for mixed lead halogen perovskites for high efficiency solar cells, Energy Environ. Sci. 9 (2016) 1706–1724, https://doi.org/10.1039/c6ee00030d.

[7] M. Saliba, T. Matsui, J.-Y. Seo, K. Domanski, J.-P. Correa-Baena, M.K. Nazeeruddin, S.M. Zakeeruddin, W. Tress, A. Abate, A. Hagfeldt, M. Grätzel, Cesium Containing Triple Cation Perovskite Solar Cells: Improved Stability, Rreproducibility and High Efficiency, Energy Environ. Sci. 9 (2016) 1989.

[8] H. Min, D.Y. Lee, J. Kim, G. Kim, K.S. Lee, J. Kim, M.J. Paik, Y.K. Kim, K.S. Kim, M. G. Kim, T.J. Shin, S. Il Seok, Perovskite solar cells with atomically coherent interlayers on SnO2 electrodes, Nature 598 (7881) (2021) 444–450.

[9] F. Giustino, H.J. Snaith, Toward lead-free perovskite solar cells, ACS Energy Lett. 1 (6) (2016) 1233–1240.

[10] N.K. Noel, S.D. Stranks, A. Abate, C. Wehrenfennig, S. Guarnera, A.-A. Haghighirad, A. Sadhanala, G.E. Eperon, S.K. Pathak, M.B. Johnston, A. Petrozza, L.M. Herz, H.J. Snaith, Lead-free organic–inorganic tin halide perovskites for photovoltaic applications, Energy Environ. Sci. 7 (9) (2014) 3061–3068.

[11] R. Ali, G.-J. Hou, Z.-G. Zhu, Q.-B. Yan, Q.-R. Zheng, G. Su, Stable mixed group II (Ca, Sr) and XIV (Ge, Sn) lead-free perovskite solar cells, J. Mater. Chem. A. 6 (2018) 9220–9227, https://doi.org/10.1039/C8TA01490F.

[12] L. Qian, Y. Sun, M. Wu, C. Li, D. Xie, L. Ding, G. Shi, A lead-free two-dimensional perovskite for a high-performance flexible photoconductor and a light-stimulated synaptic device, Nanoscale 10 (2018) 6837–6843, https://doi.org/10.1039/C8NR00914G.

[13] E.S. Parrott, R.L. Milot, T. Stergiopoulos, H.J. Snaith, M.B. Johnston, L.M. Herz, Effect of Structural Phase Transition on Charge-Carrier Lifetimes and Defects in CH3NH3SnI3 Perovskite, J. Phys. Chem. Lett. 7 (2016) 1321–1326, https://doi.org/10.1021/acs.jpclett.6b00322.

[14] X. Lu, Z. Zhao, K. Li, Z. Han, S. Wei, C. Guo, S. Zhou, Z. Wu, W. Guo, C.L. Wu, First-principles insight into the photoelectronic properties of Ge-based perovskites, RSC Adv. 6 (2016) 86976–86981, https://doi.org/10.1039/C6RA18534G.

[15] M. Lyu, J.H. Yun, M. Cai, Y. Jiao, P.V. Bernhardt, M. Zhang, Q. Wang, A. Du, H. Wang, G. Liu, L. Wang, Organic–inorganic bismuth (III)-based material: A lead-free, air-stable and solution-processable light-absorber beyond organolead perovskites, Nano Res. 9 (2016) 692–702, https://doi.org/10.1007/s12274-015-0948-y.

[16] R.L.Z. Hoye, R.E. Brandt, A. Osherov, V. Stevanovic, S.D. Stranks, M.W.B. Wilson, H. Kim, A.J. Akey, J.D. Perkins, R.C. Kurchin, J.R. Poindexter, E.N. Wang, M.G. Bawendi, V. Bulovic, T. Buonassisi, Methylammonium Bismuth Iodide as a Lead-Free, Stable Hybrid Organic-Inorganic Solar Absorber, Chem. - A Eur. J. 22 (2016) 2605–2610, https://doi.org/10.1002/chem.201505055.

[17] K. Ahmad, S.N. Ansari, K. Natarajan, S.M. Mobin, Design and Synthesis of 1D-Polymeric Chain Based [(CH3NH3)3Bi2Cl9] n Perovskite: A New Light Absorber Material for Lead Free Perovskite Solar Cells, ACS Appl. Energy Mater. 1 (2018) 2405–2409, https://doi.org/10.1021/acsaem.8b00437.

[18] P. Chandra, S.K. Mandal, Morphology controlled (CH3NH3)3Bi2Cl9 thin film for lead free perovskite solar cell, Physica B 625 (2021), https://doi.org/10.1016/j.physb.2021.413536 413536.

[19] A. Suzuki, H. Okada, T. Oku, Role of bromine doping on the photovoltaic properties and microstructures of CH3NH3PbI3 perovskite solar cells, AIP Conf. Proc. 1709 (2016), https://doi.org/10.1063/1.4941221 020022.

[20] A. Suzuki, H. Okada, T. Oku, Fabrication and Characterization of CH3NH3PbI3−x−yBrxCly Perovskite Solar Cells, Energies 9 (2016) 376, https://doi.org/10.3390/en9050376.

[21] A.M.A. Leguy, J.M. Frost, A.P. McMahon, V.G. Sakai, W. Kochelmann, C. Law, X. Li, F. Foglia, A. Walsh, B.C. O'Regan, J. Nelson, J.T. Cabral, P.R.F. Barnes, The dynamics of methylammonium ions in hybrid organic-inorganic perovskite solar cells, Nat. Commun. 6 (2015), https://doi.org/10.1038/ncomms8124.

[22] A. Oranskaia, J. Yin, O.M. Bakr, J.-L. Brédas, O.F. Mohammed, Halogen Migration in Hybrid Perovskites: The Organic Cation Matters, J. Phys. Chem. Lett. 9 (2018) 5474–5480, https://doi.org/10.1021/acs.jpclett.8b02522.

[23] Z. Wang, C. Jiang, R. Huang, H. Peng, X. Tang, Investigation of Optical and Photocatalytic Properties of Bismuth Nanospheres Prepared by a Facile Thermolysis Method, J. Phys. Chem. C 118 (2013) 1155–1160, https://doi.org/10.1021/jp4065505.

[24] C. Bedoya-Hincapie, M. Pinzón Cárdenas, E. Alfonso, E. Restrepo Parra, J. Florez, Physical-chemical properties of bismuth and bismuth oxides: synthesis, characterization and applications, DYNA. 79 (2012) 139–148.

[25] H.-B. Fu, J.-N. Yao, Size Effects on the Optical Properties of Organic Nanoparticles, J. Am. Chem. Soc. 123 (2001) 1434–1439, https://doi.org/10.1021/ja0026298.

[26] M.R. Das, A. Mukherjee, P. Mitra, Structural, optical and electrical characterization of CBD synthesized CdO thin films: influence of deposition time, Mater. Sci.-Poland 35 (2017) 470–478, https://doi.org/10.1515/msp-2017-0063.

[27] L. Zhang, Z.-J. Tang, Polaron relaxation and variable-range-hopping conductivity in the giant-dielectric-constant material Ca Cu 3 Ti 4 O 12, Phys. Rev. B 70 (2004) 174306.

[28] M. Venkateswarlu, K. Narasimha Reddy, B. Rambabu, N. Satyanarayana, A.c. conductivity and dielectric studies of silver-based fast ion conducting glass system, Solid State Ion. 127 (2000) 177–184, https://doi.org/10.1016/S0167-2738(99)00257-X.

[29] R.J. Sengwa, P. Dhatarwal, S. Choudhary, Study of time-ageing effect on the ionic conduction and structural dynamics in solid polymer electrolytes by dielectric relaxation spectroscopy, Solid State Ion. 324 (2018) 247–259, https://doi.org/10.1016/j.ssi.2018.07.015.

[30] P. Chandra, S. Saha, S.K. Mandal, A dielectric study of Br-doped lead-free methylammonium bismuth chloride (CH3NH3)3Bi2BrxCl9−x, Appl. Phys. A. 128 (2022) 541, https://doi.org/10.1007/s00339-022-05677-9.

[31] A. Molak, M. Paluch, S. Pawlus, J. Klimontko, Z. Ujma, I. Gruszka, Electric modulus approach to the analysis of electric relaxation in highly conducting (Na0. 75Bi0. 25)(Mn0. 25Nb0. 75) O3 ceramics, J. Phys. D: Appl. Phys. 38 (2005) 1450.

[32] B.H. Venkataraman, K.B.R. Varma, Frequency-dependent dielectric characteristics of ferroelectric SrBi2Nb2O9 ceramics, Solid State Ion. 167 (2004) 197–202.

[33] H. Yamamura, S. Takeda, K. Kakinuma, Dielectric relaxations in the Ce1−xNdxO2− δ system, Solid State Ion. 178 (2007) 1059–1064.

[34] I. Belkyal, R. Mokhlisse, B. Tanouti, K.-F. Hesse, W. Depmeier, Low-Temperature Phase Transition and Structural Relationships of (CH3NH3) 3Bi2Cl9, J. Solid State Chem. 155 (2000) 286–291, https://doi.org/10.1006/jssc.2000.8886.

[35] N. Onoda-Yamamuro, T. Matsuo, H. Suga, Calorimetric and IR spectroscopic studies of phase transitions in methylammonium trihalogenoplumbates (II)†, J. Phys. Chem. Solids 51 (1990) 1383–1395, https://doi.org/10.1016/0022-3697(90)90021-7.